NASA/TM–2006-214548

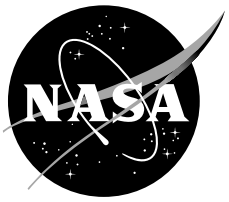

Techniques for Surface-Temperature Measurements and Transition Detection on Projectiles at Hypersonic Velocities—Status Report No. 2

D. W. Bogdanoff
Eloret, Sunnyvale, California, 94087

M. C. Wilder
Ames Research Center, Moffett Field, California 94035-1000

September 2006

The NASA STI Program Office . . . in Profile

Since its founding, NASA has been dedicated to the advancement of aeronautics and space science. The NASA Scientific and Technical Information (STI) Program Office plays a key part in helping NASA maintain this important role.

The NASA STI Program Office is operated by Langley Research Center, the Lead Center for NASA's scientific and technical information. The NASA STI Program Office provides access to the NASA STI Database, the largest collection of aeronautical and space science STI in the world. The Program Office is also NASA's institutional mechanism for disseminating the results of its research and development activities. These results are published by NASA in the NASA STI Report Series, which includes the following report types:

- TECHNICAL PUBLICATION. Reports of completed research or a major significant phase of research that present the results of NASA programs and include extensive data or theoretical analysis. Includes compilations of significant scientific and technical data and information deemed to be of continuing reference value. NASA's counterpart of peer-reviewed formal professional papers but has less stringent limitations on manuscript length and extent of graphic presentations.

- TECHNICAL MEMORANDUM. Scientific and technical findings that are preliminary or of specialized interest, e.g., quick release reports, working papers, and bibliographies that contain minimal annotation. Does not contain extensive analysis.

- CONTRACTOR REPORT. Scientific and technical findings by NASA-sponsored contractors and grantees.

- CONFERENCE PUBLICATION. Collected papers from scientific and technical conferences, symposia, seminars, or other meetings sponsored or cosponsored by NASA.

- SPECIAL PUBLICATION. Scientific, technical, or historical information from NASA programs, projects, and missions, often concerned with subjects having substantial public interest.

- TECHNICAL TRANSLATION. English-language translations of foreign scientific and technical material pertinent to NASA's mission.

Specialized services that complement the STI Program Office's diverse offerings include creating custom thesauri, building customized databases, organizing and publishing research results . . . even providing videos.

For more information about the NASA STI Program Office, see the following:

- Access the NASA STI Program Home Page at *http://www.sti.nasa.gov*

- E-mail your question via the Internet to help@sti.nasa.gov

- Fax your question to the NASA Access Help Desk at (301) 621-0134

- Telephone the NASA Access Help Desk at (301) 621-0390

- Write to:
  NASA Access Help Desk
  NASA Center for AeroSpace Information
  7121 Standard Drive
  Hanover, MD 21076-1320

NASA/TM–2006-214548

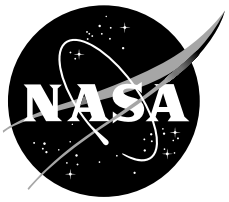

Techniques for Surface-Temperature Measurements and Transition Detection on Projectiles at Hypersonic Velocities—Status Report No. 2

D. W. Bogdanoff
Eloret, Sunnyvale, California, 94087

M. C. Wilder
Ames Research Center, Moffett Field, California 94035-1000

National Aeronautics and
Space Administration

Ames Research Center
Moffett Field, California 94035-1000

September 2006

Acknowledgments

The projectiles were fabricated by J. B. Scott. The projectiles were launched and the shadowgraphs and time data were taken by the gunners D. M. Holt, D. B. Bowling, R. E. Smythe, and ballistic range manager C. J. Cornelison. Numerous very valuable suggestions that helped us solve projectile and sabot problems were made by the machinists, the gunners, and the range manager. The shadowgraphs were developed by J-P. Wiens. Much of the shadowgraph reading and projectile position analysis was done by J. D. Brown. D. C. Reda, the project leader, offered many valuable suggestions that contributed to the success of the project. Support by NASA (Contract NAS-2-99092) to Eloret is gratefully acknowledged.

Available from:

NASA Center for AeroSpace Information
7121 Standard Drive
Hanover, MD 21076-1320
(301) 621-0390

National Technical Information Service
5285 Port Royal Road
Springfield, VA 22161
(703) 487-4650

TECHNIQUES FOR SURFACE-TEMPERATURE MEASUREMENTS AND TRANSITION DETECTION ON PROJECTILES AT HYPERSONIC VELOCITIES—STATUS REPORT NO. 2

D. W. Bogdanoff* and M. C. Wilder**

Ames Research Center

ABSTRACT

The latest developments in a research effort to advance techniques for measuring surface temperatures and heat fluxes and determining transition locations on projectiles in hypersonic free flight in a ballistic range are described. Spherical and hemispherical titanium projectiles were launched at muzzle velocities of 4.6–5.8 km/sec into air and nitrogen at pressures of 95–380 Torr. Hemisphere models with diameters of 2.22 cm had maximum pitch and yaw angles of 5.5–8 degrees and 4.7–7 degrees, depending on whether they were launched using an evacuated launch tube or not. Hemisphere models with diameters of 2.86 cm had maximum pitch and yaw angles of 2.0–2.5 degrees. Three intensified-charge-coupled-device (ICCD) cameras with wavelength sensitivity ranges of 480–870 nm (as well as one infrared camera with a wavelength sensitivity range of 3 to 5 microns), were used to obtain images of the projectiles in flight. Helium plumes were used to remove the radiating gas cap around the projectiles at the locations where ICCD camera images were taken. ICCD and infrared (IR) camera images of titanium hemisphere projectiles at velocities of 4.0–4.4 km/sec are presented, as well as preliminary temperature data for these projectiles. Comparisons were made of normalized temperature data for shots at ~190 Torr in air and nitrogen and with and without the launch tube evacuated. Shots into nitrogen had temperatures ~6% lower than those into air. Evacuation of the launch tube was also found to lower the projectile temperatures by ~6%.

* Senior Research Scientist, Eloret, Sunnyvale, California, 94087.

** Aerospace Engineer, Ames Research Center, Moffett Field, California, 94035-1000.

This document was presented at the 57th Meeting of the Aeroballistic Range Association, Sept. 18–22, 2006, Venice, Italy.

INTRODUCTION

Modeling of roughness-dominated transition is a critical design issue for thermal protection systems (TPSs). Ablating TPSs, for single-use planetary-entry and Earth-return missions, first experience recession under high-altitude, low-Reynolds-number conditions. Such laminar-flow ablation causes the formation of a distributed surface microroughness pattern characteristic of the TPS material composition and fabrication process. These roughness patterns create disturbances within the laminar boundary layer flowing over the surface. As altitude decreases, Reynolds number increases and flow-field conditions capable of amplifying these roughness-induced perturbations are eventually achieved and transition to turbulent flow occurs. Boundary-layer transition to turbulence results in higher heat-transfer and ablation rates than would be expected from laminar flow conditions (refs. 1, 2).

In order to better understand this process, ballistic-range nosetip-transition experiments were carried out with graphite and carbon/carbon composite materials in the 1970s (refs. 2–8). Nosetip surface-temperature contours were measured for each shot using cameras sensitive to visible and near infrared (NIR) radiation. This technique allowed the determination of the transition-front contour and the mean transition-front location. A nondimensional correlation involving surface roughness, surface temperature, average transition-front location, and the free-stream environment was developed; it successfully correlated wind tunnel and ballistic range data (refs. 9–13). Quantitative heat-flux information can be obtained from surface-temperature measurements by solving the unsteady one-dimensional heat-conduction equation in the bulk material under the surface. Accurate heat-flux measurements can be used to establish heat-transfer correlations for laminar and turbulent flow. The correlations then can be used to validate computational-fluid-dynamics (CFD) codes used for entry-vehicle design.

An effort was started in 2001, at the NASA Ames Research Center (ARC), to implement and further develop these earlier ballistic-range transition and heat-transfer measurement techniques in order to support current and future Earth- and planetary-entry studies. Further, using new-technology cameras (refs. 14, 15), surface-temperature measurements down to 400 K could be measured, and this was not possible during the studies of the 1970s. References 16–19 reported the initial phase of the effort—which began by validating the technique by reproducing the 1970s results. These references discussed range and gun operating conditions, the design of graphite-tipped projectiles, projectile dynamics, and the use of helium plumes to remove the glowing gas cap in front of the projectile. Projectile images obtained in the Ames Hypervelocity Free-Flight Aerodynamics Facility (HFFAF) showing transition fronts were presented in references 16–19.

Because of several difficulties in working with graphite nose projectiles, polished Ti models were used for the 2006 effort. The preferred method for preroughening the graphite projectile surface is through laminar ablation in an arcjet, but this is time-consuming and expensive. An alternative approach is to mechanically roughen the model surface by bead blasting. The latter method has been used for many of the models studied in references 16–19. The surface roughness has been measured on several sectioned models, but still is somewhat imperfectly known and not necessarily constant from projectile to projectile. The surface roughness is determined in part by the intrinsic grain size of the graphite and in part by the machining and bead-blasting operations during the fabrication of

the projectile. While emission of graphite dust from the projectile nose during flight down the range has been reduced by special cleaning techniques described in reference 18, it has not been entirely eliminated. Finally, the graphite contains on the order of 1% of CH compounds and, upon heating, these compounds can vaporize and produce a blowing effect at the projectile surface that cannot readily be characterized. The polished Ti projectiles, on the other hand, permit the results to be compared directly with classical theoretical models and experimental results for laminar-stagnation-point flow over a smooth surface (refs. 20–22). At a later point in the program with titanium models, it is planned to add roughness elements of various heights (or depths) and diameters to verify how large individual and groups of roughness elements have to be to initiate transition.

There are several potential problems that the present effort must address in order to establish that testing with titanium models is a viable technique. The models used in the 1970s work (refs. 2–8), carried out at the Arnold Engineering Development Center (AEDC), were, with only three exceptions, fired in a track range—that is, after exiting the gun muzzle, the projectiles flew along a system of four rails that maintained the projectile attitude. The free-flying graphite-tipped models used in the earlier studies in the HFFAF at the Ames Research Center were bore-rider projectiles—that is, no sabots were used and the projectile is one piece, with a graphite/steel nose screwed into a nylon after body that rides along the bore of the gun during launch. The titanium projectiles of the present effort are sabot launched. It was necessary to establish that sufficiently small maximum pitch and yaw angles can be obtained using the sabot-launched free-flying titanium projectiles. If the maximum pitch and yaw angles were too large, the heat-flux input that the projectile nose receives will be smeared over considerable distances and the heat-flux values calculated from surface temperature measurements will be degraded, as will the definition of transition locations. Further, it was necessary to establish that, using our cameras, there is a sufficient temperature difference between the temperature where the radiation from the projectile nose becomes visible and the projectile ignition temperature to allow useful heat-transfer and transition data to be taken. This paper addresses these issues.

This paper describes the work with smooth titanium spheres and hemispheres. First the range and the gun operating conditions are discussed, followed by discussion of projectile designs. The next section presents data on the pitch and yaw angles, oscillation wavelengths, and ignition characteristics for the sphere and hemisphere projectiles. Then the wavelength sensitivities of the cameras used to photograph the projectiles are discussed, and the calibration techniques for the cameras are described. Finally, representative photographs and preliminary surface-temperature data are presented.

RANGE AND GUN OPERATING CONDITIONS

Free-flying, sabot-launched projectiles were used for the present study (in contrast to the bore-rider, or track-range projectiles used in earlier studies). These projectiles must be aerodynamically stable, and it is desirable to have maximum pitch and yaw angles less than 5–6 degrees. Larger pitch and yaw angles would result in substantial smearing of the heat-flux input to the projectile, as mentioned earlier. The present effort was carried out using the largest two-stage gun available at the Ames Research Center, with a bore diameter of 3.81 cm. The diameters of most of the the titanium sphere

and hemisphere projectiles were 2.22 cm. The last two hemisphere projectiles launched had diameters of 2.86 cm.

Figure 1 is a sketch of the Ames HFFAF, showing the gun, muzzle blast dump tank, sabot stripper, the test section proper with 16 orthogonal shadowgraph stations, and the catch butt. The distance from the gun muzzle to the first station is 10 m and the spacing between the stations is 1.52 m. The distance from the gun muzzle to the last station is 33 m. Three ICCD cameras and one IR camera take nearly head-on images of the projectile, using mirrors as shown in the figure. The figure shows two cameras taking pictures at stations 7 and 15. There is also a third ICCD camera at station 11 and an IR camera at station 1; these latter cameras image the projectile at stations 11 and 1 using mirrors in the same manner as shown in figure 1 for stations 7 and 15.

Representative launch conditions for the titanium projectiles were as follows:

- Ames 3.81 cm/15.88 cm light gas gun
- Pump tube volume: 426,000 cm^3
- Powder type: IMR/Dupont 4227 booster charge (200 grams); Hercules HC-33-FS main charge
- Powder mass (total): 1750–2200 grams
- Piston mass: 21.3 kg
- Piston material: high-density polyethylene
- Piston velocity: 487–559 m/sec
- Hydrogen pressure: 4.71 bar
- Break valve rupture pressure: 172–241 bar
- Projectile mass: 43–61 grams
- Muzzle velocity: 4.6–5.8 km/sec

PROJECTILE AND SABOT DESIGNS

Cross-sections of projectiles that were launched are shown in figure 2. The projectiles were made of a common titanium alloy, Ti-6Al-4V. Titanium was chosen in part for its low thermal conductivity (relative to most other metals), which allows the projectiles to heat up sufficiently in the flight down the range to make the thermal radiation from the projectile surface readily visible to the ICCD cameras. Titanium also has the advantage (compared to, for example, Inconel and Hastelloy) of a wider range between the temperature at which the radiation is visible in the ICCD cameras and the melting or ignition temperature of the metal. According to reference 23, in air, titanium has an ignition temperature of ~1870 K at 1 atm pressure and ~1420 K at 34 atm pressure. For most shots, test stagnation-point pressures range between 23 and 46 atm.

The sphere and hemisphere projectiles in figures 2(a) and 2(b) had diameters of 2.22 cm; later on in the program, hemispheres with diameters of 2.86 cm (fig. 2(c)) were used to improve spatial resolution. The sphere models had a small pin at the aft extremity of the projectile so that pitch and yaw angles could be determined. All projectiles were fabricated from commercially available spheres. The surface roughness of the spheres, according to the manufacturer's specifications, was 5 microinches. The sphere models were drilled and tapped and the aft pin was then threaded in

place. The hemispheres were made by sectioning the commercial spheres using wire electric-discharge-machining (EDM) techniques.

The projectiles are launched using a four-finger, serrated edge sabot system as shown in the figure. The sabot material used was Acrylonitrile-Butadiene-Styrene (ABS). There were no problems in obtaining good launches.

PROJECTILE DYNAMICS AND IGNITION

Since our projectiles are flying free, the maximum pitch and yaw angles must be maintained within the previously mentioned 5–6 degree limit to avoid excessive smearing out of the heat-flux input to the projectile. In general, in the region just beyond the muzzle, the projectile receives a torque-time impulse due to nonaxisymmetric expansion of the muzzle blast gas. The projectile then exits the muzzle blast region with the pitch and yaw angles increasing at certain rates produced by the impulse. Assuming that the projectile is statically stable, after it leaves the muzzle region with the given pitch rate, it will execute approximately sinusoidal motions in pitch and yaw angle (ignoring damping) because of aerodynamic restoring forces. The maximum pitch or yaw angle reached can be shown to vary linearly with the initial pitch/yaw rate and the wavelength of the oscillation (ref. 16). Hence, the maximum pitch or yaw angle can be reduced by either reducing the torque-time impulse at the muzzle (i.e., reducing the initial pitch or yaw rate) or by increasing the aerodynamic restoring force, thereby shortening the wavelength of the pitch oscillation. Steps taken to reduce disturbances at the muzzle are described in reference 16. Hemispheres are very stable statically and should behave as just described. Spheres have, ideally, zero static stability and thus, given initial pitch and yaw rates, the pitch and yaw angles of a sphere would be expected to continually increase as the projectile flies down the range.

Key operating parameters and results for the present series of 12 shots are given in table 1. The last column gives the Reynolds number at the gun muzzle. The table contains data for two 2.22-cm-diameter sphere shots, eight 2.22-cm-diameter hemisphere shots, and two 2.86-cm-diameter hemisphere shots. For a given projectile and given initial pitch or yaw rates at the muzzle, simple theoretical analyses (ref. 16) predict that both the maximum pitch and yaw angles and the wavelength of the pitch and yaw oscillations vary as the range pressure to the –0.5 power. For the hemisphere projectiles for which data are shown in table 1, figure 3 shows the maximum absolute pitch or yaw angle (whichever is greater) plotted versus the range pressure. The data for titanium projectiles is divided into three classes—2.22-cm-diameter hemispheres fired through a diaphragm from an evacuated launch tube, 2.22-cm-diameter hemispheres fired with the launch tube not evacuated, and 2.86-cm-diameter hemispheres (“large hemispheres”). Figure 3 also shows data for 13 graphite nose hemisphere nose models and 21 graphite nose 70-degree sphere cone models, which are discussed later in this section. (Results for the graphite nose models were presented in some detail in refs. 16–19.) Figure 4 is an enlarged version of figure 3 showing only the data for the titanium models. Figure 5 shows, for the titanium projectiles, the oscillation wavelength versus the range pressure. These data were obtained by reading the projectile angles from the shadowgraphs

taken for each shot. Trend lines for maximum angle or wavelength versus range pressure are shown for each class of projectiles shown in figures 3–5. These trend lines have the functional form

$$(\text{Angle}) \text{ or } (\text{Wavelength}) = A(\text{Range pressure})^{B}.$$

TABLE 1. KEY OPERATING PARAMETERS AND RESULTS FOR SHOTS OF THE TEST SERIES

Shot number	Type of model	Muzzle velocity (km/s)	Range gas	Range pressure (Torr)	Barrel evacuated?	Max pitch angle (deg)	Max yaw angle (deg)	Proj. ignited?	Re at muzzle
2350	Sphere	~4.7	Air	379.1	No	—	—	Yes	3.39×10^6
2351	Sphere	4.656	Air	190.8	No	24.2	18.4	No	1.69×10^6
2352	Hemisphere	4.646	Air	188.4	No	5.0	3.6	No	1.67×10^6
2353	Hemisphere	4.676	Air	152.0	No	4.7	2.0	No	1.35×10^6
2354	Hemisphere	4.547	Air	152.0	Yes	7.2	3.2	No	1.32×10^6
2355	Hemisphere	4.521	Air	191.1	Yes	5.8	4.0	No	1.64×10^6
2356	Hemisphere	4.700	Air	94.8	No	7.0	3.3	No	0.85×10^6
2357	Hemisphere	4.711	N2	190.0	No	6.0	1.9	No	1.71×10^6
2358	Hemisphere	5.799	Air	94.9	Yes	8.0	4.2	Yes	1.05×10^6
2359	Hemisphere	4.670	N2	190.1	Yes	1.6	5.5	No	1.69×10^6
2360	Large hemi.	4.736	Air	190.5	Yes	2.0	0.7	Yes	2.21×10^6
2361	Large hemi.	4.689	N2	94.9	No	2.5	1.8	No	1.09×10^6

A 6-degree maximum pitch or yaw angle corresponds to a peak-to-peak motion of the heat-flux pattern on the projectile nose of ~11% of the projectile diameter. Reference 24 gives plots of heat flux versus angle from the stagnation point for hypersonic flow over a hemisphere. From these plots, the percentage peak-to-peak variations of heat transfer for a maximum pitch or yaw angle of 6 degrees (12 degrees peak to peak) are 8%, 15%, and 23% for angular displacements from the stagnation point of 20, 30, and 40 degrees, respectively. The changes in the average heat-transfer rates due to the angular motion are much less, about 2%. These variations were judged to be acceptable. The variation of heat flux exactly at the sphere or hemisphere nose is much less sensitive to pitch or yaw angles than at distances of 20–40 degrees from the projectile nose. Measurements of heating exactly at the projectile nose can tolerate pitch and yaw angles up to 8–10 degrees without producing errors more than 2% in the stagnation-point heat flux.

We first discuss the results for the sphere models listed in table 1. The first sphere model ignited, essentially blinding the light sheets used to trigger the shadowgraph stations so that no usable shadowgraphs were obtained for this shot. For the next sphere shot, the pressure was halved, the projectile did not ignite, and good shadowgraphs were obtained. The pitch angle for the sphere increased continuously from 6 degrees at shadowgraph station 1 to 24 degrees at station 13. The yaw angle increased continuously from 5 degrees at shadowgraph station 1 to 18 degrees at station 13,

confirming the expected zero static stability and large pitch and yaw angles of the sphere model. Hence, for the 2006 program, sphere models were abandoned after shot 2351.

Figure 3 shows that the hemisphere nose graphite projectiles have much smaller maximum angles than the 70-degree sphere cone graphite nose projectiles. (Note that the graphite nose projectiles were never fired with the launch tube evacuated, because this necessitates a diaphragm at the muzzle and the graphite is too delicate to shoot through the diaphragm.) The 2.22-cm-diameter titanium hemisphere models fired with the launch tube evacuated have roughly the same trend line for maximum angles as the graphite hemisphere nose models. To focus on the differences among the titanium hemisphere models, refer to figure 4, which shows that the 2.22-cm-diameter titanium hemisphere models fired with the launch tube at range pressure have maximum angles about 1 degree less than those fired with the launch tube evacuated. Three out of 4 shots with the launch tube at range pressure have maximum angles of 6 degrees or less, while only 2 out of 4 shots with the launch tube evacuated have maximum angles less than 6 degrees. The difference may be due to disturbances to the muzzle flow by the tubes that are required to evacuate the launch tube or to effects of the projectile passing through the diaphragm that must be used at the muzzle when the launch tube is evacuated. The two shots with 2.86-cm-diameter hemispheres show much smaller maximum angles (2–2.5 degrees vs. 5–8 degrees) than the 8 shots with 2.22-cm-diameter hemispheres. This is believed to be due to larger mass and moment of inertia of the 2.86-cm-diameter projectiles relative to the sabot when compared to the 2.22-cm-diameter projectiles. In other words, the initial pitch and yaw rates that the sabot can give to the projectile upon separation are much smaller for the larger projectiles.

The slopes of the power-law fits shown in figures 3 and 4 vary considerably from the ideal theoretical value (–0.5). For the titanium projectiles, the slopes vary from –0.32 to –0.50. The simple theoretical model presented in reference 16 assumes that the initial pitch and yaw rates given to a given model do not change with range pressure. This assumption may not be a good one. Also, some of the datasets of figures 3 and 4 have very large scatter and/or may be too small to give reliable exponents. The exponents of the power-law fits for figure 5 are –0.29 for the 2.22-cm-diameter projectiles and –0.82 for the 2.86-cm-diameter projectile, but the latter dataset contains only 2 points. The –0.29 exponent is smaller than expected for the 8 data point set, but this dataset still may have too few points to give a good value for the exponent.

For three of the shots of table 1, the projectile ignited. For shot number 2350, the range pressure was twice that of any other shot, and for shot number 2358, the muzzle velocity was 1 km/sec faster than for any other shot, although the range pressure was relatively low. Hence, there were clear reasons for these projectiles to ignite, because of very high convective heating. For shot 2360, the reason for ignition was less obvious. Based on temperature data for numerous shots, the projectile of shot 2360 should not have ignited. However, this was a shot with the launch tube evacuated and hence the projectile was fired through a diaphragm. The IR camera image indicates ignition at a small spot on the projectile. A possibility is that a piece of the diaphragm material may have stuck to the projectile and thus created a roughness element that led to transition, increased heat flux, and hence ignition of the projectile at that location.

Excluding shot number 2350 at a range pressure of 379.1 Torr, in which the projectile ignited and no velocity data were obtained, the Reynolds numbers of the projectiles, based on diameter and muzzle velocity, range from 0.85×10^6 to 2.21×10^6.

SURFACE TEMPERATURE MEASUREMENT TECHNIQUE

Elimination of Shock-Layer Radiation

The surface temperatures of the projectiles were determined by measuring the thermal radiation from the titanium surface. While flying through air in the range, the projectile nose is surrounded by a cap of very hot radiating gas (i.e., the shock layer), which adds to the radiation from the titanium surface. The radiating gas cap must be stripped away when the ICCD camera photographs are taken to allow accurate determination of the titanium surface temperature. This stripping was done by passing the projectile through small regions where most of the air in the range is replaced by helium. In the current set-up, the projectile flies mostly through air, but through ~20-cm-diameter vertical plumes of helium where the three ICCD camera picture are taken.

The helium plumes are produced by "chimneys" (fig. 6). Helium is introduced into the bottom of the chimney, which has a diameter of ~20 cm and a height of ~30 cm. The helium passes through various flow-restricting elements to produce nearly uniform flow at the exit of the chimney. Further details of the chimney operation and experimental verification of the effectiveness of the helium plume in eliminating the gas-cap radiation are presented in reference 18. For the 3–5 micron wavelength range IR camera, it was determined that there was no need to use a helium plume to strip away the gas-cap radiation.

Imaging Systems and Optical Setup

The projectiles were photographed using three Roper Scientific (ref. 14) PI.MAX:512HQ ICCD cameras. These cameras have a 512 x 512 imaging array and a wavelength sensitivity of roughly 480 to 900 nm. Exposure times of 1 microsec were used in order to "freeze" the motion of the projectile. The projectiles were viewed from angles of 10 to 15 degrees away from head-on, using expendable first-surface mirrors. These cameras were set up to photograph the projectile just downstream of shadowgraph stations 7, 11, and 15. An Indigo (ref. 15) Phoenix mid-IR camera with a 320 x 256 InSb imaging array was used for temperatures lower than those detectable using the ICCD cameras. The ICCD cameras used Nikon Nikkor 180-mm f/2.8 lenses at f/8. The IR camera used a Janos Technology Asio series 100-mm f/2.3 lens (3–5 micron), a 3–5 micron band-pass filter, and an IR neutral-density filter. (Densities of 1, 2, or 3 were used, depending upon the shot.) With the IR camera, a 15-cm-diameter clear-aperture silicon window is used in the range so that the full wavelength range of the camera can be used. This camera also viewed the projectiles nearly head-on, using expendable mirrors. It was set up to take photographs at shadowgraph station 1 in the ballistic range.

The Roper Scientific cameras were calibrated using two black-body furnace sources that can reach temperatures up to 1470 and 3270 K. The optical system used during the calibrations was set up the same way as the optical system used to take data in the range. The emissivity of the titanium alloy in the temperature range of interest is roughly 0.6. The cameras had maximum counts/pixel of 65,535 (16 bit) and typical dark noise levels of ~100 counts/pixel. Above 1200 K in the calibration, the uncertainty in the temperature ranged from 2 to 7 K. For lower temperatures, the uncertainty is higher, but as long as the camera signal is greater than ~2% of full scale, the uncertainty in temperature is less than 10 K. These uncertainties were determined experimentally, based on noise levels, during the furnace calibrations.

The optical setup in the range for the ICCD camera at shadowgraph station 7 is shown in figure 7. (The muzzle blast dump tank is located between the gun muzzle and shadowgraph station 1, but it is not shown in the figure.) The projectile is shown at two different times in its trajectory. When the projectile passes through the light beam at stations 6 (not shown in the figure) and 7, pulses are produced in the photocell output. From the timing of these two pulses, using an up-down counter and the known distances along the range, a third pulse can be produced when the projectile should be the center of the plume from the helium chimney. This pulse is used to trigger the ICCD camera. A nearly identical setup is used at stations 11 and 15 to take two more ICCD camera images. For the IR camera, no helium plume is used and the image is taken directly at station 1, without any trigger delay. (At the IR wavelengths, the gas-cap radiation is extremely low compared to the radiation from the titanium surface, as mentioned previously.) The view shown in figure 7 is from the side of the range. The light beam and helium chimney are shown as they actually are, but, for clarity, the optical path for the camera is shown rotated into the vertical plane; it is actually in the horizontal plane.

ICCD AND IR IMAGES OF PROJECTILES, PRELIMINARY TEMPERATURE FIELD DATA

Figure 8 shows the four camera images taken in shot 2353, a shot of a 2.22-cm-diameter titanium hemisphere into 152 Torr air. The muzzle velocity was 4.68 km/sec and the Reynolds number at the muzzle was 1.35×10^6. The image of figure 8(a) was taken with the IR camera, and the remaining three images were taken with the ICCD cameras. The exposure times were 8 microsec for the IR camera and 1 microsec for the ICCD cameras. Figures 8(a), 8(b), 8(c), and 8(d) were taken at shadowgraph stations 1, 7, 11, and 15, respectively. In the ICCD images, the wake is clearly visible to the left of the projectile. For figure 8(b), the bright spots are believed to be dust kicked up by the shock wave and are located well behind the projectile.

Figure 9 shows normalized temperature plots for the four images shown in figure 8. All temperatures were normalized by the stagnation-point temperature at station 15. Because the camera used at station 11 had not yet been calibrated, the temperature data of figure 9(c) were obtained by applying the calibration of the camera at station 15 to the raw-image data obtained at station 11.

Table 2 shows the normalized projectile stagnation temperatures for shots 2352, 2357, and 2359. The data are normalized by the highest temperatures measured at the station in question for shot 2352.

TABLE 2. NORMALIZED STAGNATION TEMPERATURES FOR SHOTS 2352, 2357, AND 2359.

Shot number	Range gas	Barrel evacuated?	Normalized stagnation temperature at station 11	Normalized stagnation temperature at station 15
2352	Air	No	1.000	1.000
2357	Nitrogen	No	0.941	0.929
2359	Nitrogen	Yes	0.895	0.873

All data are for 2.22-cm-diameter titanium hemispheres. The range fill pressures varied only slightly for these three shots, from 188.4 to 190.1 Torr. Likewise, there were only slight variations in the muzzle velocity for these shots, from 4.646 to 4.711 km/sec. These variations of 0.9 to 1.4% are incapable of explaining the variations in temperatures between shots shown in table 2. However, the variations of temperatures correspond to whether the test gas was air or nitrogen and whether the launch tube was evacuated or not.

Neither shot 2352 nor shot 2357 had the launch tube evacuated, but shot 2352 was fired into air while shot 2357 was fired into nitrogen. The temperatures for shot 2352 were 6–7% higher than those for shot 2357, believed to be due to surface catalysis of oxygen recombination reactions not present in nitrogen atmosphere shots. Calculations indicate that, for test conditions, nearly all the oxygen is dissociated while only ~20% (by mole fraction) of nitrogen is dissociated. Both shots 2357 and 2359 were fired into nitrogen, but the launch tube was evacuated for shot 2359 and was not evacuated for shot 2357. The temperatures for shot 2359 were 5–6% lower than those for shot 2357. It is believed that heating in the launch tube was responsible for this difference.

As mentioned previously, lower temperatures were obtained using an evacuated launch tube, indicating in-launch-tube heating when the launch tube is not evacuated. Unfortunately, as noted in the section on projectile dynamics and ignition, tests with the launch tube evacuated produced larger maximum pitch and yaw angles than those with the launch tube not evacuated. (Possible reasons for this were discussed in that section.) A possible alternative solution to the in-launch-tube heating problem would be not to evacuate the launch tube, but to use a sabot design that totally encloses the projectile. This technique was used in reference 25.

SUMMARY AND CONCLUSIONS

The most recent developments in a research effort to advance techniques for determining transition location and measuring surface temperatures and heat fluxes on projectiles in hypersonic free flight in a ballistic range were described. The projectiles fired and the launcher operating conditions were discussed. The operating conditions for the Ames 3.81-cm light gas gun needed to obtain the desired launch conditions (projectile masses of 43–61 g; muzzle velocities of 4.6–5.8 km/sec) were given. The projectiles launched to date were 2.22-cm-diameter spheres and hemispheres and 2.86-cm hemispheres made of titanium Ti-6Al-4V alloy. The four-finger serrated-sabot design was discussed.

Since the projectiles were free flying, it was necessary to minimize their maximum pitch and yaw angles. The 2.22-cm-diameter projectiles had maximum pitch or yaw angles of 5.5–8 degrees and 4.7–7 degrees, depending on whether they were launched using an evacuated launch tube or not. The 2.86-cm-diameter hemisphere models had maximum pitch or yaw angles of 2–2.5 degrees. The sphere models, as expected, showed zero static stability, with pitch and yaw angles increasing continuously down the range to values of ~20 degrees at the end of the range. The maximum pitch and yaw angles and the projectile oscillation wavelength were found to decrease as the range pressure increased, as predicted theoretically. A helium chimney plume system used to remove the radiating gas cap around the projectile at the location where the ICCD camera pictures were taken was described.

A number of ICCD and infrared camera images of 2.22-cm-diameter hemisphere projectiles at velocities of 4 to 4.4 km/sec and a range pressure of ~150 Torr were presented. Preliminary normalized surface-temperature data are also shown for these pictures. Comparisons were made of normalized temperature data for shots at ~190 Torr in air and nitrogen and with and without the launch tube evacuated. Shots into nitrogen had temperatures ~6% lower than those into air. The higher temperatures in air are believed to be caused by catalytic heating due to recombination of dissociated oxygen at the projectile surface. Evacuation of the launch tube was also found to lower the projectile temperatures by ~6%.

The technique of surface-temperature and heat-transfer measurements using smooth sabot-launched titanium hemispheres at hypersonic velocities appears very promising. The maximum pitch and yaw angles obtained for the 2.22-cm-diameter hemisphere projectiles were as good as those obtained for earlier graphite-tipped projectiles. The angles obtained with the 2.86-cm-diameter hemisphere models were much smaller (2 to 2.5 degrees) than those obtained with the graphite-tipped models. A range of test conditions where the projectiles did not ignite but there was good visibility of projectile radiation to determine temperature was found. Although the use of an evacuated launch tube was found to reduce the heating of the projectile, it also created other problems. A better option to eliminate in-launch-tube heating may be to use a sabot that totally encloses the model. It appears very likely that, by the addition of roughness elements, the present technique can be used to determine the size of isolated and grouped roughness elements necessary to trigger transition at various Reynolds numbers. This step would be next one to take in the research effort.

REFERENCES

1. Reda, D. C.: Review and Synthesis of Roughness-Dominated Transition Correlations for Reentry Applications. J. Spacecraft & Rockets, vol. 39, no. 2, March–April, 2002, pp. 161–167.

2. Reda, D. C.: Correlation of Nosetip Boundary-Layer Transition Data Measured in Ballistic-Range Experiments. AIAA J., vol. 19, no. 3, March, 1981, pp. 329–339.

3. Reda, D. C.; Leverance, R. A.; and Longas, S. A.: Aerothermodynamic Testing and Analysis of Reentry Vehicle Nosetips in Hypersonics Ballistics-Range Flight. Paper presented at 22nd Intl. Instrumentation Symposium, Instrument Soc. Am., San Diego, Calif., May 1976.

4. Reda, D. C.; and Leverance, R. A.: Boundary-Layer Transition Experiments on Pre-Ablated Graphite Nosetips in a Hyperballistics Range. AIAA J., vol. 15, March 1977, pp. 305–306.

5. Reda. D. C.; and Brown, H. S.: Analysis of Nosetip Boundary-Layer Transition Data Using Interactive Graphics. Paper presented at 24th Intl. Instrumentation Symposium, Instrument Soc. Am., Albuquerque, N.M., May 1978.

6. Reda, D. C.; and Raper, R. M.: Measurements of Transition-Front Assymetries on Ablating Graphite Nosetips in Hypersonic Flight. AIAA J., vol. 17, Nov. 1979, pp. 1201–1207.

7. Reda, D. C.: Comparative Transition Performance of Several Nosetip Materials as Defined by Ballistics-Range Testing. Paper presented at 25th Intl. Instrumentation Symposium, Instrument Soc. Am., Anaheim, Calif., May 1979; also, ISA Trans., vol. 19, no. 1, 1980, pp. 83–98.

8. Norfleet, G. D.; Hendrix, R. E.; and Jackson, D.: Development of a Hypervelocity Track Facility at AEDC. AIAA Paper 77-151, 15th Aerospace Sciences Meeting, Los Angeles, Calif., Jan. 1977.

9. Anderson, A. D.: Passive Nosetip Technology (PANT) Program, Interim Report, Volume X. Appendix A: Boundary Layer Transition on Nosetips with Rough Surfaces. SAMSO-TR-74-86, Jan. 1975.

10. Dirling, R. B., Jr.; Swain, C. E.; and Stokes, T. R.: The Effect of Transition and Boundary Layer Development on Hypersonic Reentry Shape Change. AIAA Paper 75-673, 10th Thermophysics Conf., Denver, Colo., May 1975.

11. van Driest, E. R.: Evaluation of PANT Transition Roughness Data and Transition Criterion. Unpublished memo to SAMSO, Nov. 1975.

12. Finson, M. L.: An Analysis of Nosetip Boundary Layer Transition Data. AFOSR-TR-76-1106, Aug., 1976.

13. Bishop, W. M.: Transition Induced by Distributed Roughness on Blunt Bodies in Supersonic Flow. AIAA Paper 77-124, 15th Aerospace Sciences Meeting, Los Angeles, Calif., Jan. 1977.

14. User Manual 4411-0069, Version 2.A, October 18, 1999, PI-MAX Camera (Princeton Instruments), Roper Scientific, 3660 Quakerbridge Road, Trenton, N.J., 08619.

15. Technical information on Phoenix cameras from Indigo Systems Corporation, 50 Castilian, Goleta, Calif., 93117.

16. Bogdanoff, D. W.; and Reda, D. C.: Technique for Transition Measurements on Hemisphere Nose Projectiles at Hypersonic Velocities – Projectile Design and Launcher Issues. Paper presented at 53rd Meeting of the Aeroballistic Range Assoc., Sendai, Japan, Oct. 21–25, 2002.

17. Bogdanoff, D. W. and Wilder, M. C., Technique for Transition and Heat Flux Measurements on Projectiles at Hypersonic Velocities. This paper presented at 54th Meeting of the Aeroballistic Range Assoc., Santa Fe and Albuquerque, N.M., USA, Oct. 19–24, 2003.

18. Bogdanoff, D. W.; and Wilder, M. C.: Techniques for Transition and Surface Temperature Measurements on Projectiles at Hypersonic Velocities – A status Report. Paper presented at 55th Meeting of the Aeroballistic Range Assoc., Freiberg, Germany, Sept. 27–Oct. 1, 2004.

19. Reda, D. C.; Wilder, M. C.; Bogdanoff, D. W.; and Olejniczak, J: Aerothermodynamic Testing of Ablative Reentry Vehicle Nosetip Materials in Hypersonic Ballistic-Range Environments. AIAA paper AIAA-2004-6829, presented at USAF Developmental Test and Evaluation Summit, Woodland Hills, Calif., Nov. 16-18, 2004.

20. Fay, J. A.; and Riddell, F. R.: Theory of Stagnation Point Heat Transfer in Dissociated Air. J. Aeron. Sci., vol. 25, no. 2, Feb. 1958, pp. 73–85.

21. Anderson, J. D. Jr.: Hypersonic and High Temperature Gas Dynamics. McGraw-Hill (New York) 1989, pp. 626–636.

22. Zoby, E. V.: Empirical Stagnation-Point Heat-Transfer Relation in Several Gas Mixtures. NASA TN D-4799, Oct. 1968.

23. Hill, P. R.; Adamson, D.; Foland, D. H.; and Bressette, W. E.: High-Temperature Oxidation and Ignition of Metals. NACA RM L55L23b, Mar. 1956.

24. Anderson, J. D., Jr.: Hypersonic and High Temperature Gas Dynamics. McGraw-Hill (New York), 1989, p. 262.

25. Compton, D. L.; and Cooper, D. M.: Free-Flight Measurements of Stagnation-Point Convective Heat Transfer at Velocities to 41,000 ft/sec. NASA TN D-2871, June 1965.

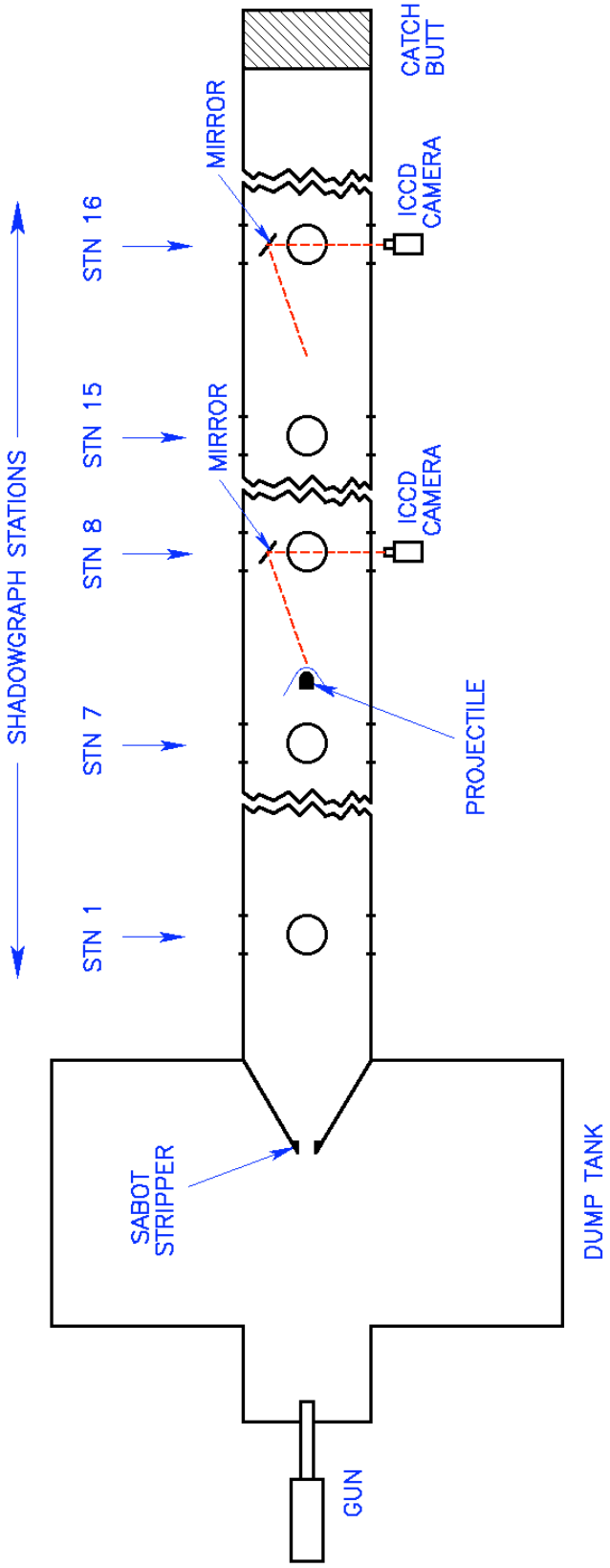

Figure 1. Ames Aerodynamic Range.

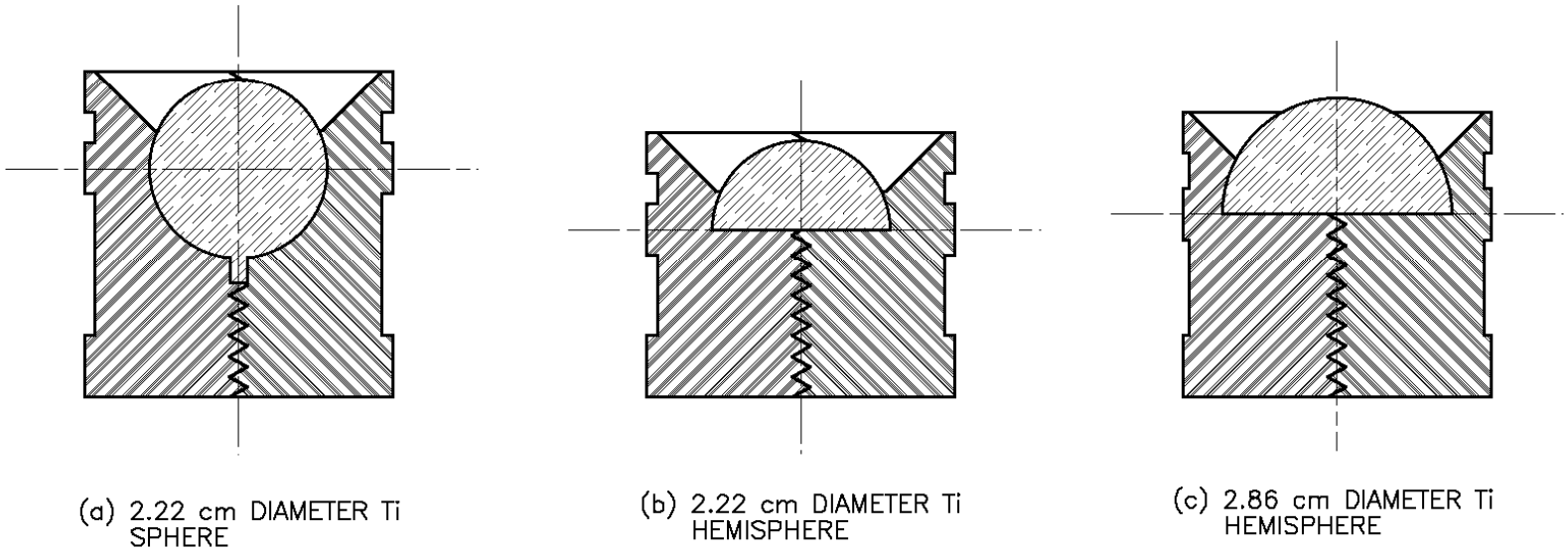

Figure 2. Projectiles launched in the present study.

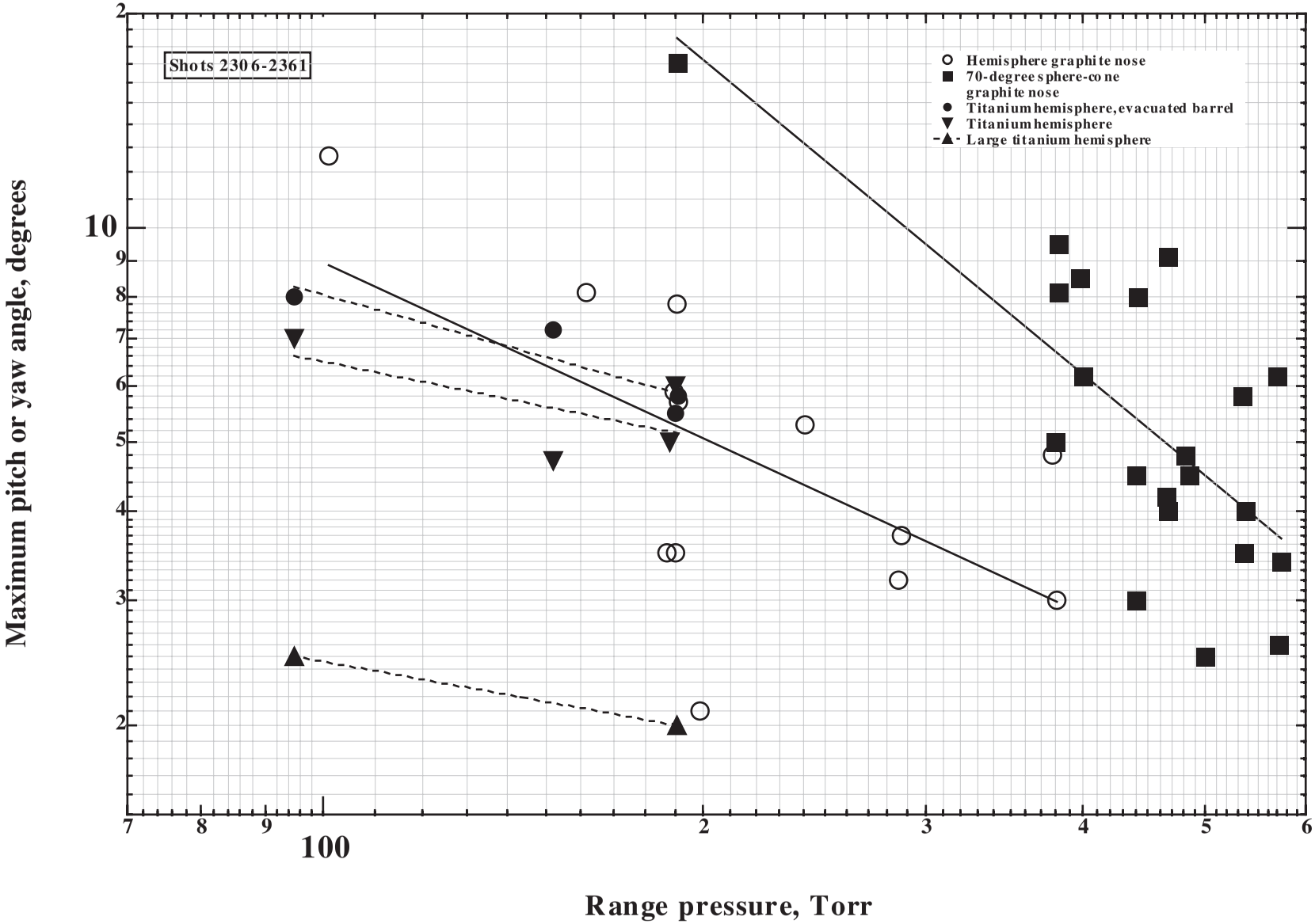

Figure 3. Maximum pitch or yaw angle vs. range pressure.

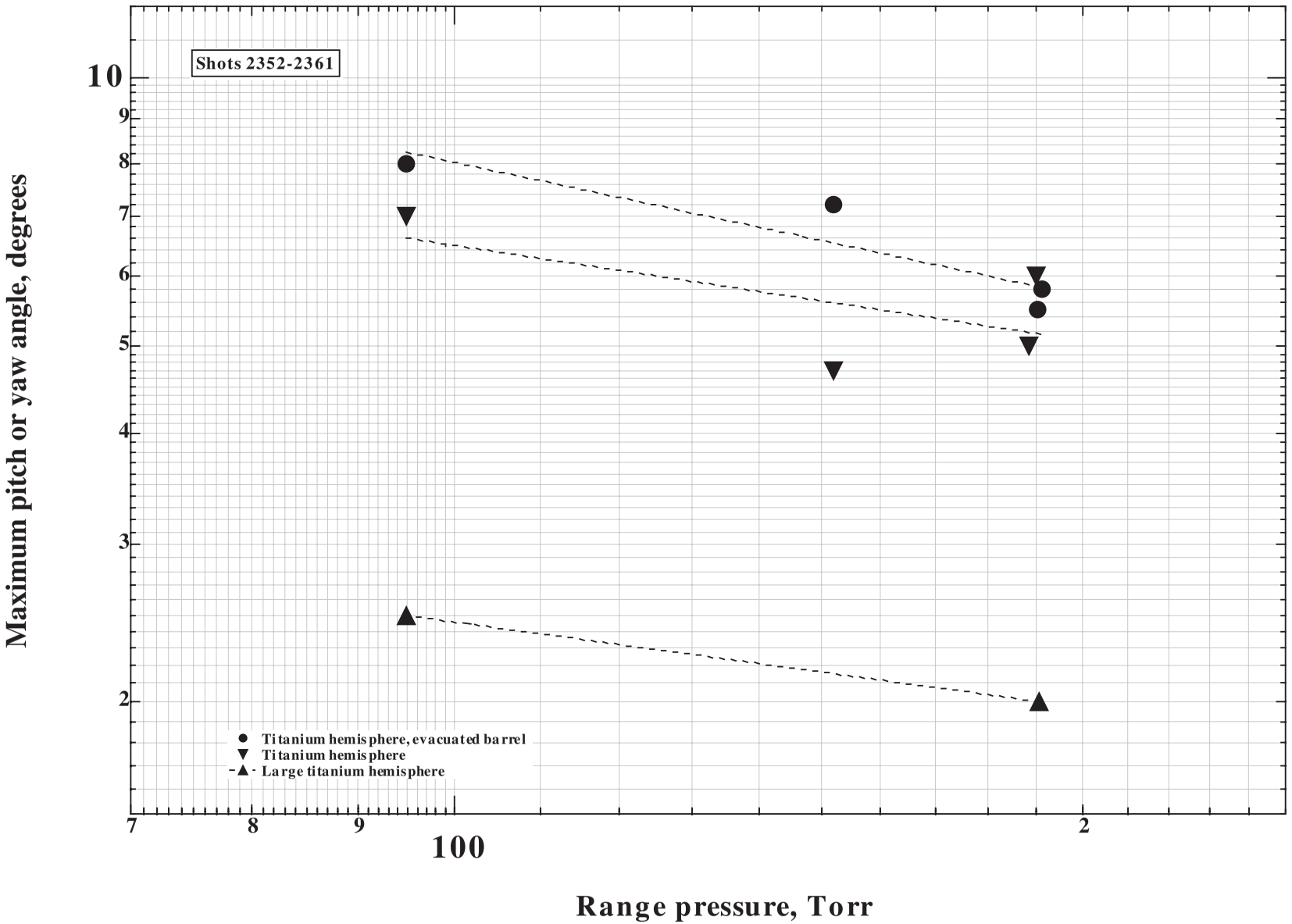

Figure 4. Maximum pitch or yaw angle vs. range pressure.

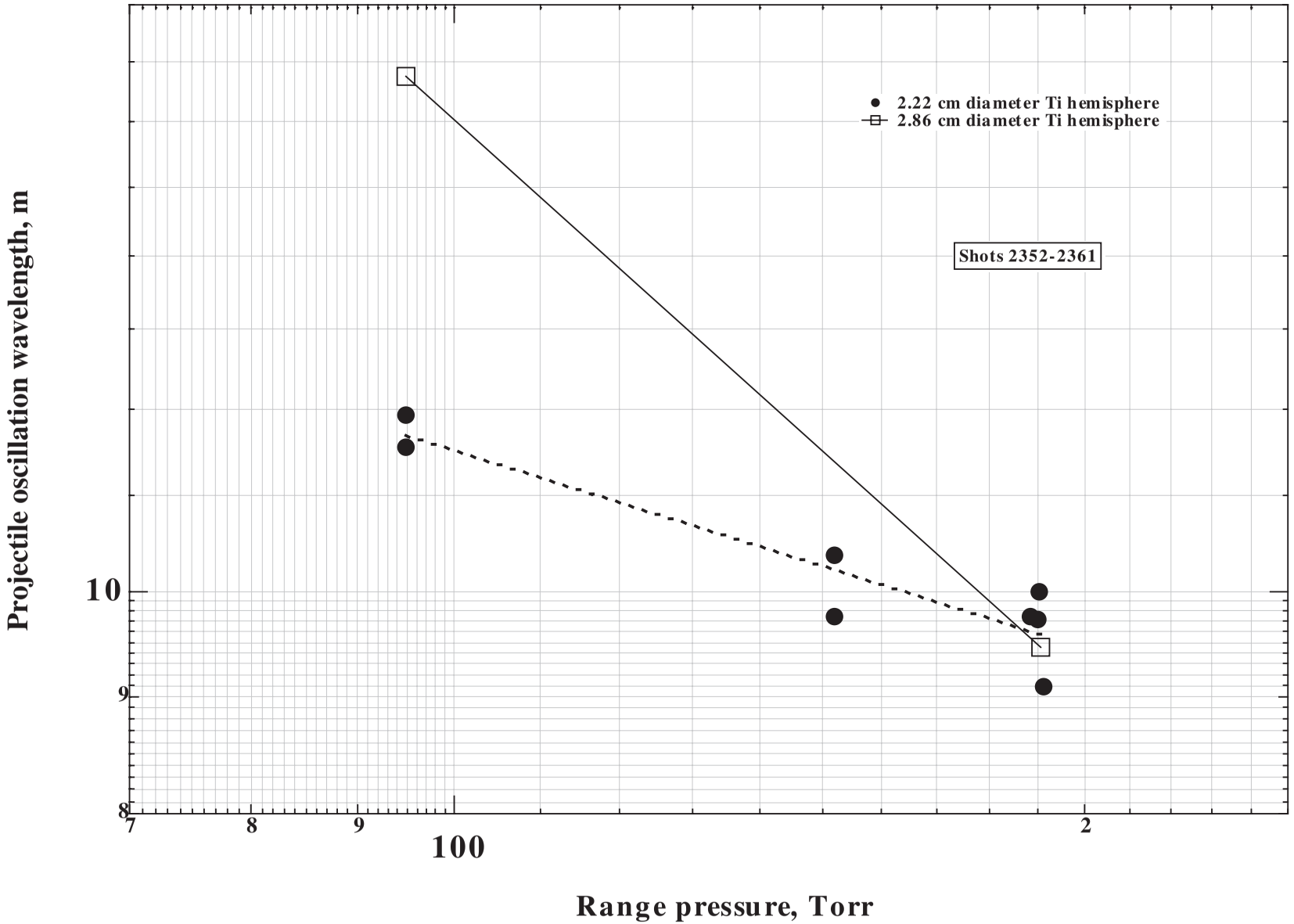

Figure 5. Oscillation wavelength of projectiles vs. range pressure.

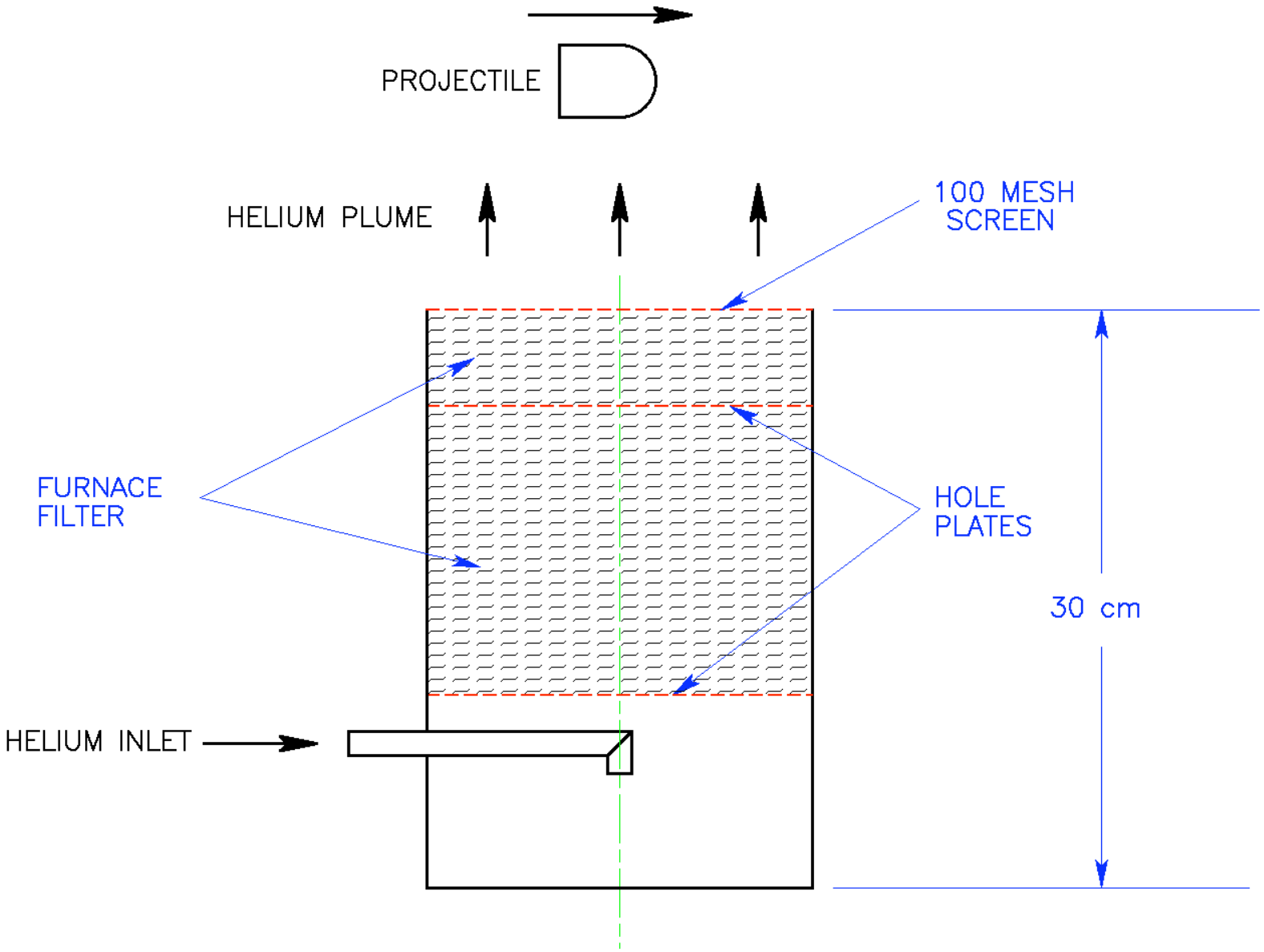

Figure 6. Helium chimney for range.

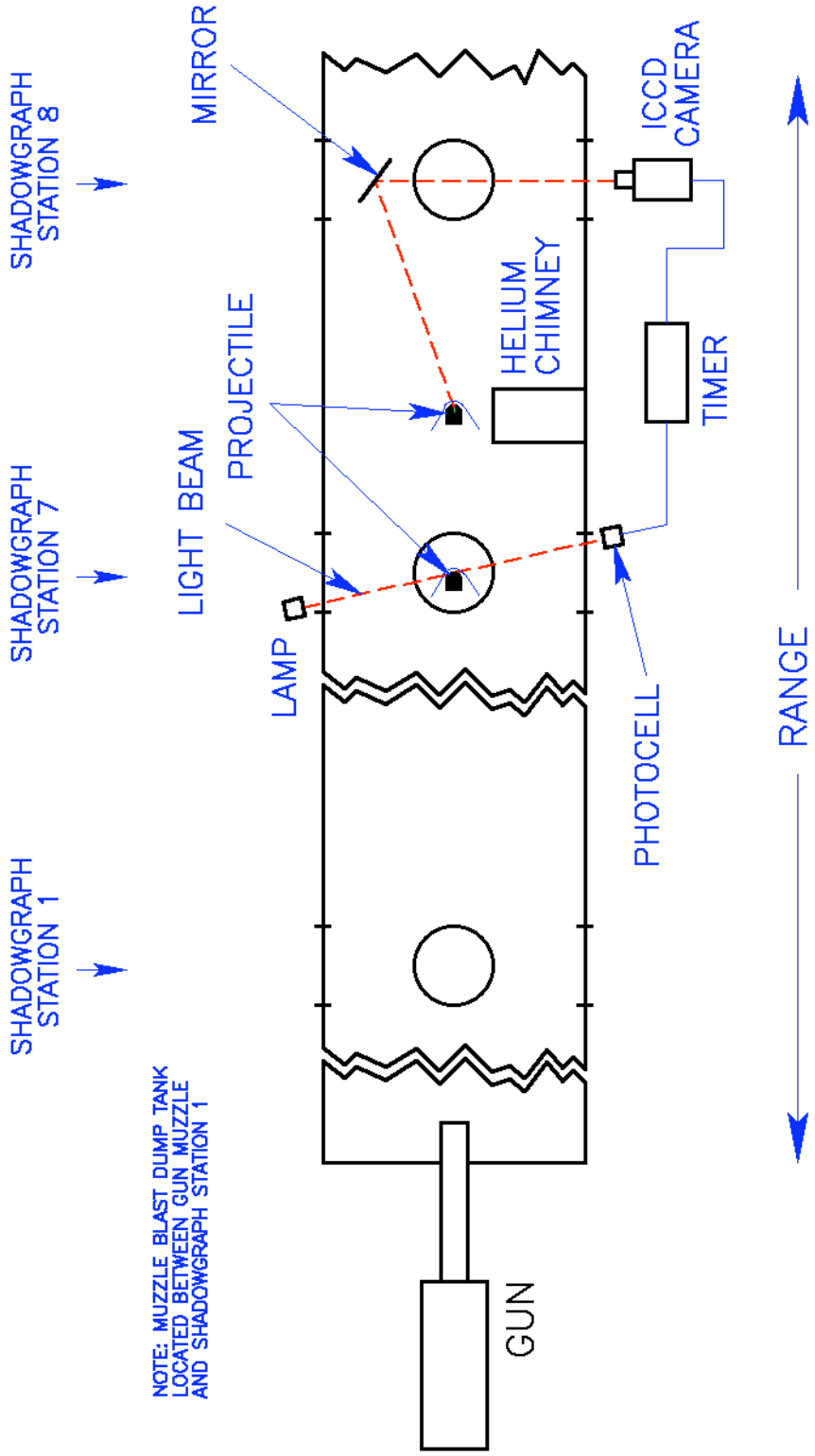

Figure 7. Typical range optical setup.

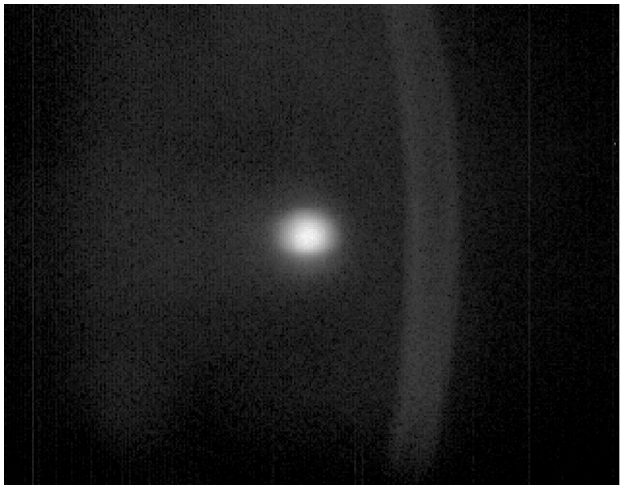

(a) Station 1, IR camera.

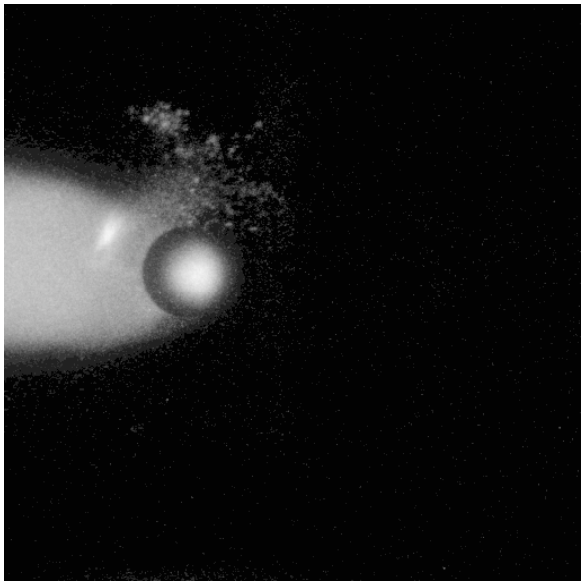

(b) Station 7, ICCD camera.

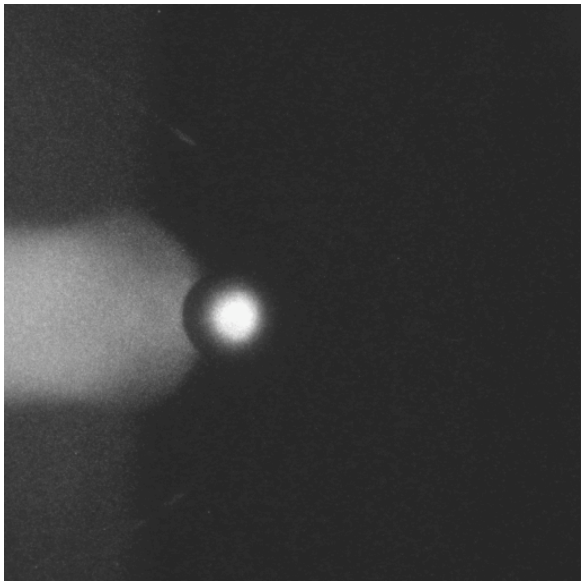

(c) Station 11, ICCD camera.

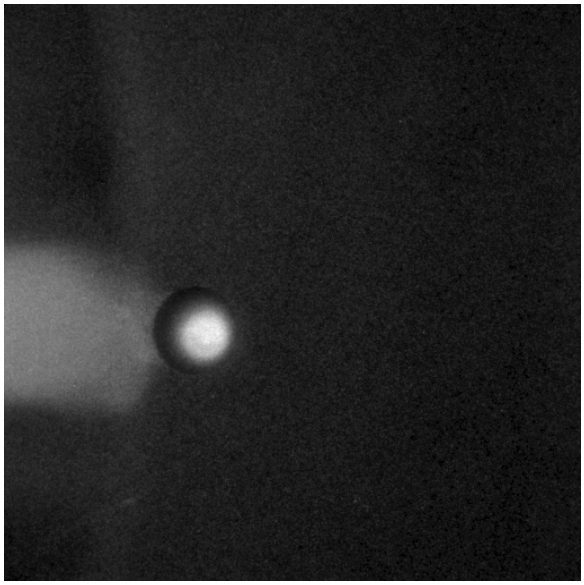

(d) Station 15, ICCD camera.

Figure 8. IR and ICCD camera images for shot 2353; 2.22-cm-diameter titanium hemisphere fired with muzzle velocity of 4.68 km/sec into air at 152 Torr pressure.

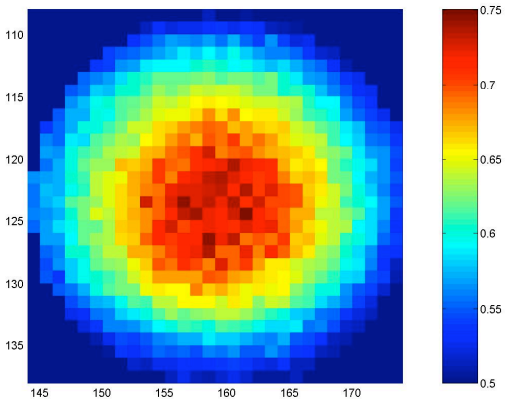

(a) Station 1, IR camera.

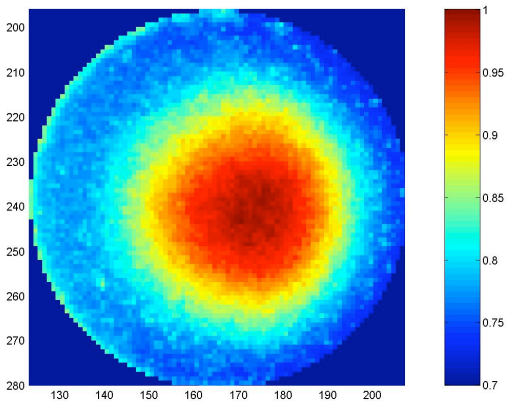

(b) Station 7, ICCD camera.

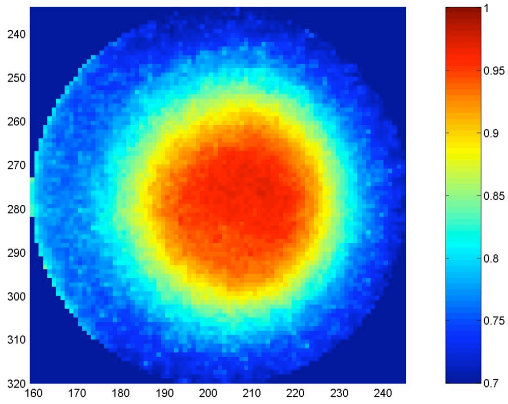

(c) Station 11, ICCD camera.

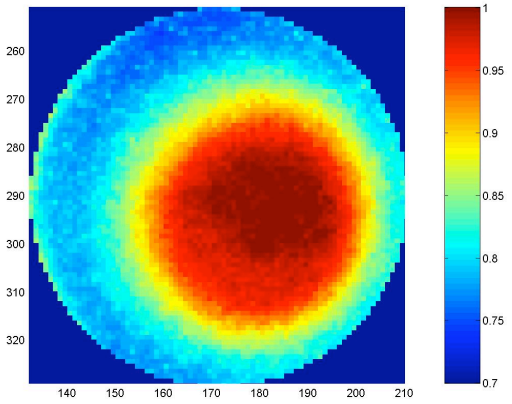

(d) Station 15, ICCD camera.

Figure 9. Normalized temperature plots for shot 2353; 2.22-cm-diameter titanium hemisphere fired with muzzle velocity of 4.68 km/sec into air at 152 Torr pressure. Temperatures normalized by stagnation point temperature at station 15.

REPORT DOCUMENTATION PAGE

Form Approved
OMB No. 0704-0188

1. REPORT DATE *(DD-MM-YYYY)*	2. REPORT TYPE	3. DATES COVERED *(From - To)*
30/09/2006	Technical Memorandum	

4. TITLE AND SUBTITLE

Techniques for Surface-Temperature Measurements and Transition Detection on Projectiles at Hypersonic Velocities—Status Report No. 2

5a. CONTRACT NUMBER

5b. GRANT NUMBER

5c. PROGRAM ELEMENT NUMBER

6. AUTHOR(S)

D. W. Bogdanoff[1] and
M. C. Wilder[2]

5d. PROJECT NUMBER

5e. TASK NUMBER

5f. WORK UNIT NUMBER
939252.05.05.02

7. PERFORMING ORGANIZATION NAME(S) AND ADDRESS(ES)

[1]Eloret, Sunnyvale, California, 94087, and
[2]Ames Research Center, Moffett Field, California 94035-1000

8. PERFORMING ORGANIZATION REPORT NUMBER
A-0600012

9. SPONSORING/MONITORING AGENCY NAME(S) AND ADDRESS(ES)

National Aeronautics and Space Administration
Washington, DC 20546-0001

10. SPONSORING/MONITOR'S ACRONYM(S)
NASA

11. SPONSORING/MONITORING REPORT NUMBER
NASA/TP–2006-214548

12. DISTRIBUTION/AVAILABILITY STATEMENT

Unclassified — Unlimited
Subject Category 14 Distribution: Nonstandard
Availability: NASA CASI (301) 621-0390

13. SUPPLEMENTARY NOTES

Point of Contact: D. W. Bogdanoff, Eloret, MS 230-2, Moffett Field, CA 94035-1000 (650) 604-6138
This document was presented at the 57th Mtg. of the Aeroballistic Range Assn. in Venice, Italy, Sept. 18–22, 2006.

14. ABSTRACT

The latest developments in a research effort to advance techniques for measuring surface temperatures and heat fluxes and determining transition locations on projectiles in hypersonic free flight in a ballistic range are described. Spherical and hemispherical titanium projectiles were launched at muzzle velocities of 4.6–5.8 km/sec into air and nitrogen at pressures of 95–380 Torr. Hemisphere models with diameters of 2.22 cm had maximum pitch and yaw angles of 5.5–8 degrees and 4.7–7 degrees, depending on whether they were launched using an evacuated launch tube or not. Hemisphere models with diameters of 2.86 cm had maximum pitch and yaw angles of 2.0–2.5 degrees. Three intensified-charge-coupled-device (ICCD) cameras with wavelength sensitivity ranges of 480–870 nm (as well as one infrared camera with a wavelength sensitivity range of 3 to 5 microns), were used to obtain images of the projectiles in flight. Helium plumes were used to remove the radiating gas cap around the projectiles at the locations where ICCD camera images were taken. ICCD and infrared (IR) camera images of titanium hemisphere projectiles at velocities of 4.0–4.4 km/sec are presented as well as preliminary temperature data for these projectiles. Comparisons were made of normalized temperature data for shots at ~190 Torr in air and nitrogen and with and without the launch tube evacuated. Shots into nitrogen had temperatures ~6% lower than those into air. Evacuation of the launch tube was also found to lower the projectile temperatures by ~6%.

15. SUBJECT TERMS

Transition, Hypervelocity projectiles, Surface temperature measurements

16. SECURITY CLASSIFICATION OF:			17. LIMITATION OF ABSTRACT	18. NUMBER OF PAGES	19a. NAME OF RESPONSIBLE PERSON
a. REPORT	b. ABSTRACT	c. THIS PAGE			D. W. Bogdanoff
Unclassified	Unclassified	Unclassified	Unclassified	26	19b. TELEPHONE *(Include area code)* (650) 604-6138